A SIMULATION AND EXPERIMENTAL STUDY ON EQUIVALENT DIPOLE LAYER IMAGING OF BRAIN ELECTRIC SOURCES

J. Lian[1], D. Yao[2], D. Wu[1,2], B. He[1,2]
Departments of [1]Bioengineering and [2]EECS, University of Illinois at Chicago, IL, USA

Abstract – **A simulation and experimental study has been conducted on equivalent dipole layer imaging (EDLI) of brain electric sources from EEG. Using the three-sphere inhomogeneous head model, the performance of the EDLI was rigorously evaluated for a variety of brain source configurations under different noise levels. The present simulation results demonstrate the excellent performance of the EDLI in mapping and imaging the underlying cortical sources with much enhanced spatial resolution, as compared to the scalp potentials. Human experiments were further conducted to examine the feasibility of EDLI. Pattern reversal visual evoked potentials (VEP) were recorded from 94 electrodes and the brain electric sources at P100 were estimated. The VEP experiments demonstrate that the present EDLI can eliminate the misleading far field in the scalp potential map, localize and map the underlying cortical sources induced by the visual stimuli.**

Keywords: **forward problem, inverse problem, equivalent dipole layer imaging, VEP**

I. INTRODUCTION

Although conventional EEG offers excellent temporal resolution in resolving rapidly changing pattern of brain electric activities, its spatial resolution is limited by the smoothing effect of the head volume conductor, especially due to the very low conductivity skull layer [1].

A number of investigators have attempted to improve the spatial resolution of the EEG by solving the EEG inverse problem [2-13]. Of particular interest is the recently developed cortical imaging technique (CIT) [7-13], in which an explicit biophysical model of the passive conducting properties of a head is used to deconvolve a measured scalp potential distribution into a potential distribution on the cortical surface. The CIT needs to construct a virtual dipole layer (DL) inside the cortical surface and a closed DL equivalently represents all the brain electric sources bounded by its surface [10-13]. The inverse procedure estimates the equivalent DL from the scalp EEG, then the cortical potentials are reconstructed by solving the forward problem, from the estimated equivalent DL to the cortical potentials [7-13].

Although as an intermediate result of CIT, the estimate of the DL may also facilitate the equivalent representation of brain electric sources, previous CIT approaches had to further calculate the cortical potentials, due to the lack of the forward theory on the equivalent DL. Recently, we have proposed the equivalent dipole layer imaging (EDLI), which provides, for the first time, the forward theory of the equivalent DL. Based on this theory, the brain electric sources can be directly imaged on the equivalent DL from EEG measurements, thus eliminating the need for the forward calculation of cortical potentials in the CIT. In the present study, we conducted both computer simulations and human experiments to rigorously evaluate the performance of EDLI and its feasibility to image brain activation.

II. METHODS

A. Forward solution of the equivalent DL

Considering an arbitrary-shaped head model as illustrated in Fig. 1, where S' represents the scalp surface and S represents the virtual DL. Denote V_0 as the volume bounded within S, and V the volume bounded by S and S'. If all brain electric sources are in V_0 and there is no active source in V, then for any given point x within V, the potential function $\varphi(x)$ can be expressed as [14]:

$$\varphi(x) = \oint_S [G(x,x')(\sigma \frac{\partial \varphi(x')}{\partial n'}) - (\sigma\varphi(x'))\frac{\partial G(x,x')}{\partial n'}]ds' \qquad (1)$$

where x' is on S, $\partial/\partial n'$ is the normal derivative at surface S, σ is the conductivity in V_0, $G(x,x')$ is the Green function which is the potential solution of a point current source inside a volume conductor model.

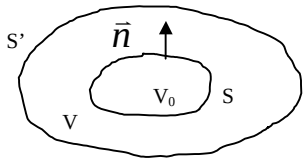

Fig. 1 Illustration of DL in an arbitrary-shaped head model

Different from the conventional Green function method [14], Eq. (1) can be solved by keeping G unchanged, while modifying function φ by decomposing it into two potential components produced by the sources in volumes V and V_0, respectively. Since the sources in volume V make no contribution to the surface integral in Eq. (1), we can replace $\varphi(x)$ with a proper $\varphi'(x)$ so that:

$$\varphi'(x') = \varphi'(x')_V + \varphi(x')_{V0}, \text{ for } x' \text{ on S} \qquad (2a)$$

$$\frac{\partial \varphi'(x')}{\partial n'} = \frac{\partial \varphi'(x')_V}{\partial n'} + \frac{\partial \varphi(x')_{V0}}{\partial n'} = 0, \text{ for } x' \text{ on S} \qquad (2b)$$

Then Eq. (1) can be simplified to:

$$\varphi(x) = \oint_S (\sigma\varphi'(x'))\frac{\partial G(x,x')}{\partial n'}ds' = \oint_S (\sigma\varphi'(x'))G_d(x,x')ds', \text{ for } x' \text{ on S} \qquad (3)$$

where $G_d = -\partial G/\partial n'$ is the Green function of a dipole on surface S oriented normally outward. Therefore, Eq. (3) can

Report Documentation Page

Report Date	Report Type	Dates Covered (from... to)
25OCT2001	N/A	-

Title and Subtitle A Simulation and Experimental Study on Equivalent Dipole Layer Imaging of Brain Electric Sources	**Contract Number**
	Grant Number
	Program Element Number
Author(s)	**Project Number**
	Task Number
	Work Unit Number
Performing Organization Name(s) and Address(es) Departments of 1Bioengineering and 2EECS, University of Illinois at Chicago, IL	**Performing Organization Report Number**
Sponsoring/Monitoring Agency Name(s) and Address(es) US Army Research, Development & Standardization Group (UK) PSC 802 Box 15 FPO AE 09499-1500	**Sponsor/Monitor's Acronym(s)**
	Sponsor/Monitor's Report Number(s)

Distribution/Availability Statement
Approved for public release, distribution unlimited

Supplementary Notes
Papers from the 23rd Annual International Conference of the IEEE Engineering in Medicine and Biology Society, October 25-28, 2001, held in Istanbul, Turkey. See also ADM001351 for entire conference on cd-rom., The original document contains color images.

Abstract

Subject Terms

Report Classification unclassified	**Classification of this page** unclassified
Classification of Abstract unclassified	**Limitation of Abstract** UU

Number of Pages
4

be considered as an equivalent DL model, with equivalent dipole source density of $f_d = \sigma\varphi'(x')$, and with Green function of G_d. Eq. (3) is valid for an arbitrary geometric model and numerical methods can be applied to calculate G_d. Specially, when the equivalent DL is considered to be a spherical surface, the closed solution of f_d can be obtained, with $\varphi'(x')$ be the surface potential produced by a dipole inside a homogeneous conducting sphere with boundary condition as described in Eq. (2a,b). This implies that f_d is proportional to the potential over the same spherical surface when the exterior space of the DL is replaced by air. In another word, the equivalent DL source density distribution may reflect the potential distribution over this layer, had the upper medium being removed during the open-skull surgery.

B. Inverse problem of EDLI

The proposed EDLI constructs the equivalent dipole source distribution over the DL, which is essentially not affected by the low-conductivity skull layer, and has higher spatial resolution as compared to the scalp potential map.

Discretize Eq. (3) as:

$$\varphi(x) = \sum_i (f_d(i)ds_i)G_d(x,x'), \text{ for } x' \text{ on S} \quad (4)$$

Denote the source density weighed by discrete grid area $f_d(i)ds_i$ as the equivalent DL source strength. Then Eq. (4) linearly relates the potential φ for x in V, with the equivalent DL source strength, by the discrete Green function G_d. Specially, when φ is the measured scalp potential, Eq. (8) can be written in matrix form:

$$\vec{\phi}_s = A\vec{F} \quad (5)$$

where $\vec{\phi}_s$ is the vector of measured scalp potentials, $\vec{F}$ is the vector of equivalent DL source strength, A is the lead field matrix obtained by evaluating G_d.

Denote the pseudo-inverse of A as A^+, the equivalent DL source strength can be estimated as:

$$\vec{F} = A^+\vec{\phi}_s \quad (6)$$

The proposed EDLI is based on the inverse estimation of vector $\vec{F}$, and the truncated singular value decomposition (TSVD) was applied to improve the numerical stability of the inverse problem [15].

C. Simulation and experimental protocols

Computer simulations based on the three-sphere inhomogeneous head model [16] were conducted to evaluate the EDLI. The normalized radii of the equivalent DL, the brain, the skull and the scalp spheres were taken as 0.80, 0.87, 0.92 and 1.0, respectively. The normalized conductivity of the scalp and the brain was taken as 1.0, and that of the skull as 0.0125. Four unit-moment dipole sources (radial or tangential) with varying eccentricity were used to represent four well-localized brain electric activity. The forward solution of the equivalent DL was validated by evaluating the relative error (RE) and correlation coefficient (CC) between the analytic cortical potentials generated by the dipoles and the cortical potentials produced by the equivalent DL. To evaluate the inverse solution of EDLI, Gaussion white noise (GWN) was added to the scalp potentials generated by the simulating dipoles to simulate noise-contaminated scalp potential measurement. The source strength of the equivalent DL was estimated using Eq. (6) and compared with the forward solution. The TSVD was applied to solve the inverse problem, and the minimal product (MINP) method was used to determine the truncation parameter in TSVD [12].

Human visual evoked potentials (VEPs) were recorded from two healthy subjects according to a protocol approved by UIC/IRB. Visual stimuli were generated by the STIM system (Neuro Scan Labs). 94-channel VEP signals referenced to right earlobe were amplified, band pass filtered and acquired by the ESI systems (Neuro Scan Labs). The electrode locations were measured using Polhemus Fastrack (Polhemus Inc.) and best fitted on the spherical surface with unit radius. Half visual field pattern reversal checkerboards with reversal interval of 0.5 sec served as visual stimuli and 400 reversals were grand averaged to get VEP signals. The EDLI maps at P100 were estimated and compared to the corresponding scalp potential maps.

III. RESULTS

A. Evaluation of the forward solution of equivalent DL

Tab.1 shows the effect of source eccentricity on the accuracy of forward solution of equivalent DL, which was discretized into 1280 grids. Four radial or tangential dipoles at $r\cdot(\pm\sin(\pi/6),0,\cos(\pi/6))$ and $r\cdot(0,\pm\sin(\pi/6),\cos(\pi/6))$ were used to simulate brain electric sources, where r is the eccentricity of the dipoles and ranges from 0.30 to 0.75. Tab. 1 clearly indicated that for both radial and tangential dipoles, very low RE and high CC values were achieved for most source eccentricities, except for r = 0.75 when sources are very close to the DL.

Tab. 1 Effect of source eccentricity (ECC)

ECC	*0.20*	*0.30*	*0.40*	*0.50*	*0.60*	*0.70*	*0.75*
RE-rad	0.0281	0.0281	0.0282	0.0290	0.0336	0.0652	0.1885
CC-rad	0.9996	0.9996	0.9996	0.9996	0.9994	0.9979	0.9842
RE-tag	0.0279	0.0278	0.0280	0.0285	0.0300	0.0463	0.1759
CC-tag	0.9996	0.9996	0.9996	0.9996	0.9996	0.9989	0.9844

Tab. 2 shows the effect of the grid density on the accuracy of forward solution of equivalent DL. Four radial or tangential dipoles (as described above) were fixed at r=0.60, and the equivalent DL was constructed with varying grid densities (320, 640, 1280, 2560, and 5120). Tab. 2 clearly revealed that for both radial and tangential dipole sources, the denser grid of the equivalent DL, the lower RE and higher CC values can be achieved.

B. Imaging brain electric sources using EDLI

Fig. 2 shows a typical example of inverse estimation of simulated brain electric sources using the EDLI approach. Fig. 2(a) displays the noise (5% GWN) contaminated scalp

Tab. 2 Effect of grid density of the equivalent DL

Grid	*320*	*640*	*1280*	*2560*	*5120*
RE-rad	0.2685	0.2009	0.0336	0.0294	0.0020
CC-rad	0.9646	0.9800	0.9994	0.9996	1.0000
RE-tag	0.2596	0.1857	0.0300	0.0243	0.0019
CC-tag	0.9670	0.9829	0.9996	0.9997	1.0000

potential map for 4 radial dipoles located at $0.7\cdot(\pm\sin(\pi/7),0,\cos(\pi/7))$ and $0.7\cdot(\pm\sin(\pi/7),0,\cos(\pi/7))$. Notably, the scalp potential map was severely blurred and distorted by the head volume conductor and additive noise. The forward solution of the EDLI and the inversely estimated EDLI maps were respectively shown in Fig. 2(b) and (c). Without the blurring effect caused by the skull layer, the EDLI maps clearly revealed the underlying dipole sources with much enhanced spatial resolution as compared to the scalp potential map, and the estimated EDLI map corresponds well to the forward solution of EDLI map.

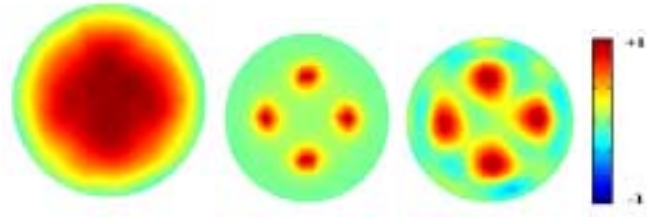

(a) (b) (c)

Fig. 2 An example of estimation of simulated brain electric sources using EDLI. All maps are normalized for display.

Fig. 3 shows the application of EDLI in VEP data analysis. Subject A and B were respecitively given left and right visual field stimuli. Their normalized scalp potential maps (top-back view) at P100 were respectively shown in Fig. 3(a) and (b), and the estimated EDLI maps (top-back view) were respectively shown in Fig. 3(c) and (d). Notably, in response to the left visual field stimuli, a dominant positive potential component was elicited with a widespread distribution on the left scalp (Fig. 3(a)). While in response to the right visual field stimuli, a widely distributed positive potential component was dominant on the right scalp (Fig. 3 (b)). On the other hand, the estimated EDLI map in response to the left visual field stimuli revealed a dominant and more localized activity in the right visual cortex (Fig. 3(c)). Consistently, the estimated EDLI map in response to the right visual field stimuli indicated a dominant and more localized activity in the left visual cortex (Fig. 3 (d)).

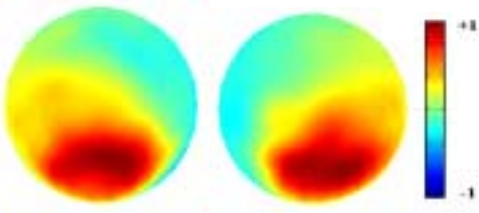

(a) (b)

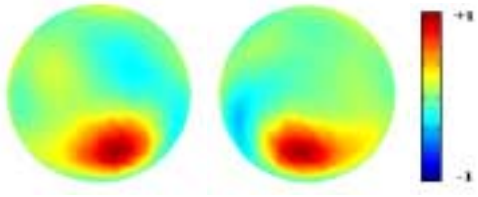

(c) (d)

Fig. 3 Application of the EDLI to VEP data analysis. All maps are normalized for display.

IV. DISCUSSION

From the point of view of electromagnetic theory, a closed surface DL can equivalently represent all the electric sources enclosed by its surface. By constructing an equivalent DL, the potential everywhere between this DL and the scalp can be determined, including the cortical potentials as in CIT [7-13]. We have recently developed the forward theory of the EDLI, and demonstrated that the equivalent DL source density is proportional to the potential over the same surface had the upper medium being removed. This has made it possible to evaluate the equivalent source distribution directly over the equivalent DL, without a further calculation of the cortical potentials as in CIT.

In the present study, using a 3-sphere inhomogeneous head model, we have evaluated the forward solution of the EDLI by computer simulations. The results indicate that the equivalent DL can well-represent the simulating dipole sources with different eccentricity and with radial/tangential orientation (Tab. 1), and denser grid of the equivalent DL yields more accurate representation of the brain electric sources (Tab. 2). We also evaluated the EDLI-based inverse problem by both computer simulations and experimental studies. As shown in Fig. 2, the estimated EDLI map corresponded well to the analytic EDLI map, and both of them clearly resolved the underlying dipole sources with much enhanced spatial resolution as compared to the noise contaminated scalp potential map. Promising results were also obtained from EDLI analysis of P100 of VEP data (Fig. 3). It is widely accepted that the half visual field stimuli activate the visual cortex on the contralateral hemisphere of the brain. But paradoxically, the half visual field stimuli elicited stronger positive potential distribution over the ipsilateral side of the scalp (Fig. 3(a)-(b)), which might be misinterpreted as ipsilateral visual cortex activation [17]. However, the estimated EDLI maps clearly indicated that the contralateral visual cortex was activated (Fig. 3(c)-(d)), thus effectively eliminated the misleading far field observed in the scalp potential.

In summary, the promising results of the present investigation suggest the EDLI approach may offer a promising alternative means of mapping spatially distributed brain electric activity noninvasively. Further improvement of the EDLI can be achieved by taking into account the realistic geometry head model and arbitrarily shaped equivalent DL.

ACKNOWLEDGEMENT

This work was supported in part by NSF CAREER Award BES-9875344.

REFERENCES

[1] P. L. Nunez, Electric field of the brain, London: Oxford University Press, 1981.
[2] R. Srebro, R.M. Oguz, K Hughlett, and P.D. Purdy, "Estimating regional brain activity from evoked potential field on the scalp", IEEE Trans. Biomed Eng., vol. 40, pp. 509-516, 1993.
[3] A. Gevins, J. Le, N. Martin, and B. Reutter, "High resolution EEG: 124-channel recording, spatial enhancement and MRI integration methods," Eletroenceph. Clin. Neurophysiol., vol. 90, pp. 337-358, 1994.
[4] P. L. Nunez, R. B. Silibertein, P. J. Cdush, R. S. Wijesinghe, A. F. Westdrop, and R. Srinivasan. "A theoretical and experimental study of high resolution EEG based on surface Laplacian and cortical imaging," Electroenceph. Clin. Neurophysiol., vol. 90, pp. 40-57,1994.
[5] G. Edlinger, P. Wach, and G. Pfurtscheller, "On the realization of an analytic high-resolution EEG," IEEE Trans. Biomed. Eng., vol. 45, pp. 736-745, 1998.
[6] B. He, Y. Wang, and D. Wu, "Estimating cortical potentials from scalp EEG's in a realistically shaped inhomogeneous head model," IEEE Trans. Biomed. Eng., vol. 46, pp. 1264-1268, 1999.
[7] R. Sidman, M. Ford, G. Ramsey, and C. Schlichting, "Age-related features of the resting and P300 auditory evoked responses using the dipole localization method and cortical imaging technique," J. Neuroscience Methods, vol. 33, pp. 22-32, 1990.
[8] B. He, Y. Wang, S. Pak, and Y. Ling, "Cortical source imaging from scalp electroencephalograms," Med. Biol. Eng. Comput., vol. 34 (Supp. I, Pt. 2), pp. 257-258, 1996.
[9] F. Babiloni, C. Babiloni, F. Carducci, L. Fattorini, C. Anello, P. Onorati, and A. Urbano, "High resolution EEG: a new model-dependent spatial deblurring method using a realistically-shaped MR-constructed subject's head model," Electroenceph. Clin. Neurophysiol., vol. 102, pp. 69-80, 1997.
[10] Y. Wang and B. He, "A computer simulation study of cortical imaging from scalp potentials," IEEE Trans. Biomed. Eng., vol. 45, pp. 724-735, 1998.
[11] B. He, "Brain electric source imaging: scalp Laplacian mapping and cortical imaging," Crit. Rev. Biomed. Eng., vol. 27, pp.149-188, 1999.
[12] J. Lian and B. He, "A minimal product method and its application to cortical imaging," Brain Topogr., vol. 13, pp. 209-217, 2001.
[13] B. He, J. Lian, K. M. Spencer, J. Dien, and E. Donchin, "A cortical potential imaging analysis of the P300 and novelty P3 components," Hum. Brain. Mapp., vol. 12, pp.120-130, 2001.
[14] J. D. Jackson, Classical electrodynamics. Second Edition, Wiley, 1975.
[15] P. C. Hansen, "Analysis of discrete ill-posed problems by means of the L-curve," SIAM Rev., vol. 34, pp. 561-580, 1992.
[16] S. Rush and D. A. Driscoll, "EEG electrode sensitivity – an application of reciprocity," IEEE Trans. Biomed. Eng., vol. 16, pp. 15-22, 1969.
[17] G. Barrett, L. Blumhardt, A. M. Halliday, E. Halliday, and A. Kriss, "A paradox in the lateralisation of the visual evoked response," Nature, vol. 261, pp. 253-255, 1976.